

# Comparison of wave and current measurements to NORA10 and NoNoCur hindcast data in the northern North Sea

Kjersti Bruserud<sup>1,2</sup> · Sverre Haver<sup>2,3</sup>

Received: 27 January 2016 / Accepted: 29 March 2016 / Published online: 22 April 2016  
© Springer-Verlag Berlin Heidelberg 2016

**Abstract** The objective of this study is to compare metocean design criteria for waves and currents based on measured and hindcast data and by that provide some insight in the expected differences. At the Norwegian Continental Shelf (NCS), the Norwegian Reanalysis Archive (NORA10) hindcast for wind and waves and the Northern North Sea Current Hindcast Study (NoNoCur) for currents are available. A comparison of NORA10 wave and NoNoCur current data to recent wave and current measurements during May 2011 to October 2015 at four locations in the northern North Sea has been done. For waves, significant wave height ( $H_s$ ), spectral peak period ( $T_p$ ), and wave direction are compared, and for currents, current speed ( $C_s$ ) and direction at two water depths. Scatter and qq-plots of  $H_s$ ,  $T_p$ , and  $C_s$  and directional roses, summary statistics, and time histories of  $H_s$  and  $C_s$  are provided. In addition, the extreme values of  $H_s$  are estimated, the conditional log-normal distribution for  $T_p$  given  $H_s$  is discussed, and the  $H_s$ - $T_p$

contour lines are established. Good agreement between NORA10 and measured wave data in the northern North Sea is demonstrated. The NORA10  $H_s$  is found to be slightly more conservative than the measured  $H_s$ . The NoNoCur data corresponds well to current measurements in the northern North Sea. However, the NoNoCur data does not correspond as good as the NORA10 data corresponds to measured data. Consequently, NORA10 can be recommended to be used for wave design criteria at NCS, while NoNoCur must be further developed and used with caution.

**Keywords** Wave measurements · NORA10 · Current measurements · NoNoCur · Northern North Sea

## 1 Introduction

Metocean design criteria for wind, waves, and currents based on high-quality metocean data reduce uncertainties, both in design and operation of offshore structures, wind power plants, and pipelines. Reduced uncertainties result in higher safety levels of the structures and consequently reduced risks. In addition, this often leads to reduced conservatism and with that cost-saving. Thus, reliable metocean design criteria for wind, waves, and currents are essential in the design and operation of offshore structures.

During the last decades, wind and wave models have improved and consequently the quality of available wind and wave hindcast data. For the northeast Atlantic Ocean, e.g., the ERA-Interim reanalysis (Dee et al. 2011), the Norwegian Reanalysis Archive (NORA10) hindcast (Reistad et al. 2011), the Global Reanalysis of Ocean Waves (GROW2012) (Oceanweather Inc. 2016), and NEXTRA hindcast (Francis 1987; Oceanweather Inc. 2014; Peters et al. 1993) are widely used. Some current hindcasts are also available, but the quality

---

Responsible Editor: Diana Greenslade

---

This article is part of the Topical Collection on the *14th International Workshop on Wave Hindcasting and Forecasting in Key West, Florida, USA, November 8–13, 2015*

---

✉ Kjersti Bruserud  
kjbrus@statoil.com

Sverre Haver  
sverre.k.haver@uis.no

<sup>1</sup> Statoil ASA, Forusbeen 50, 4035 Stavanger, Norway

<sup>2</sup> Institute of Marine Technology, Norwegian University of Science and Technology (NTNU), Otto Niensens vei 10, 7491 Trondheim, Norway

<sup>3</sup> Department of Mechanical and Structural Engineering and Materials Science, University of Stavanger, Kjell Arholms gate 41, 4036 Stavanger, Norway

of these is generally not as good as for the wind and wave hindcasts. When wave and wind hindcast data, validated against and found to compare well with measurements, exist, these are often preferred to measured data when establishing metocean design criteria, due to long periods of continuous data.

For the Norwegian Continental Shelf (NCS), the NORA10 hindcast for wind and waves is both used and advocated to be used by Statoil when metocean design criteria for wind and waves at NCS are to be established. Metocean design criteria for wind and waves based on both NORA10 hindcast data and measurements at all locations with available measurements have been estimated, compared thoroughly, and generally found to agree very well. However, the NORA10 wind speed exceeding 15 m/s is somewhat unconservative. As these results have not been published yet and no other open references focused on metocean design criteria are available, it would be valuable and desirable to have such a reference supporting the conclusion that NORA10 could be used when establishing metocean design criteria for the NCS.

Validations of NORA10 are available (e.g., Aarnes et al. 2012; Furevik and Haakenstad 2012; Reistad et al. 2011), but none of these focuses specifically on validation of NORA10 for establishing metocean design criteria for offshore structures. Reistad et al. (2011) described the technical details of how the NORA10 hindcast has been developed. A comparison of NORA10 hindcast data to measurements, satellite observations, and ERA-40 hindcast data (Dee et al. 2011; Uppala et al. 2005) at several coastal and offshore locations was also done. Statistics related to the goodness and validation of the hindcast were compared, i.e., as mean, standard deviation, rms difference, correlation coefficient, and percentiles of wind velocity at 10 m height and significant wave height and mean wave period. Improvements were found for NORA10 over ERA-40, when these hindcasts were compared to measurements. Furevik and Haakenstad (2012) discussed the boundary layer wind speed between 10 and 150 m from NORA10 and wind measurements at both on- and offshore locations. The emphasis in this paper was also on validation of hindcast, and parameters such as mean, rms, and correlation of wind velocities were considered. The NORA10 model was found to underestimate the mean wind speed from measurements at offshore platforms with 5 to 10 %. Aarnes et al. (2012) used NORA10 to study the extreme significant wave height, based on different statistical models commonly used to establish extreme value statistics. The qualitative differences between the models were investigated, and no comparison of estimated extreme values of significant wave height to available measurements was done.

Recently, the Northern North Sea Current Hindcast Study (NoNoCur) has been completed (Danish Hydraulic Institute 2012). This current hindcast incorporates the latest

advancements in the model physics and computational capacity and as such represents the state of the art when compared to alternative current hindcast databases. No validations or comparisons of this hindcast to measured current data have been published.

This article presents a comparison of metocean design criteria for offshore structures based on NORA10 and NoNoCur hindcast data and recent wave and current measurements during May 2011 to October 2015 at four locations in the northern North Sea. The main objective of this study is to provide insight in the uncertainties related to metocean design criteria based on hindcast data over measured data. In this part of the northern North Sea, the offshore structures are mainly jackets, and for a jacket, the governing load process is the hydrodynamic load caused by waves and current. Hence, metocean design criteria for waves and currents will be compared. Wind is not considered in the following. The wave parameters, significant wave height ( $H_s$ ), spectral peak period ( $T_p$ ), and mean wave direction, are considered. The current parameters, current speed ( $C_s$ ) and direction at two different water depths, are included for the comparison. In order to give a general overview of how well hindcast and measured data compare, scatter diagrams, qq-plots, and time histories of corresponding measured and hindcast data are given. The main metocean design and operational criteria, such as summary statistics and directional roses of  $H_s$  and  $C_s$ , extreme  $H_s$ , conditional distributions of  $T_p$  given  $H_s$ , and  $H_s$ - $T_p$  contour lines, are established and compared.

This article is outlined as follows: first the measured and hindcast data are described, then the comparisons of measured and hindcast data are presented, and lastly, the conclusions are given.

## 2 Data

Several wind, wave, and current measurements and hindcast data are available at the NCS. Measurements are performed to industry standard. Thus, measured environmental data are often taken as ground truth and used as reference data. However, there are also uncertainties related to measurements. Wind measurements are very dependent on the location and the surroundings where they are made. In general, wave measurements give good descriptions of  $H_s$  and  $T_p$ , but in extreme weather conditions, they are also associated with uncertainties. Recently, the quality of current measurements, especially in the upper part of the water column, has been questioned (Bruserud and Haver, 2016, Current measurements in the northern North Sea, unpublished). Following this, three phases of the project Current Verification Study (CurVeS) have been carried out. With the last phase to be completed in Q2 2016, results will be published in the near future. Wind and wave hindcast data

generally compare well with corresponding measurements and are considered to be of good quality, but the current hindcast data are of varying quality. Here, the NORA10 hindcast for waves and the recently completed NoNoCur hindcast for currents are compared to measurements at four locations in the northern North Sea.

### 2.1 Norwegian Reanalysis Archive wave hindcast

The NORA10 hindcast is a regional hindcast for the northeast Atlantic, including the North Sea, the Norwegian Sea, and the Barents Sea, developed by the Norwegian Meteorological Institute (Aarnes et al. 2012; Reistad et al. 2011).

The hindcast is a dynamical downscaling of the global reanalysis, European Reanalysis project (ERA-40) (Dee et al. 2011; Uppala et al. 2005), using the High Resolution Limited Area Model version 6.4.2 on a 10–11-km grid (HIRLAM10) (Undén et al. 2002). For wave generation, a modified version of the wave modeling (WAM) cycle 4 model (Günther et al. 1992; Komen et al. 1996; The Wamdi Group 1988) is run on rotated longitude/latitude grid, consisting of a coarse 50-km resolution model forced by ERA-40 wind fields and a nested 10–11-km resolution model forced by HIRLAM10 winds. The model domains are indicated in Fig. 1. The model output of hindcast data is 3 h. In principle, this model output gives the conditions at that exact point of time, i.e., not any sort of 3 h averaging. In practice, due to the temporal resolution of the wind field forcings and the spatial resolution of the wave model, the hindcast data is assumed to represent a 1-h mean value. This is supported by NORA10  $H_s$  found to fit hourly  $H_s$  measurements best (personal communication with Magnar Reistad at the Norwegian Meteorological Institute).

The ERA-40 dataset covers the period from September 1957 to August 2002, which is the original period of NORA10. However, NORA10 is extended continuously based on downscaling of operational analyses by the European Centre for Medium-Range Weather Forecasts (ECMWF) and updated with a delay of approximately 2 months. The period of NORA10 data available for this study is September 1957 through June 2015. The data is assumed to be homogenous through the entire period, although the data quality has probably improved somewhat with time as more measured meteorological data have become available during the last decades.

### 2.2 Northern North Sea Current Hindcast Study

NoNoCur is a hindcast of currents, sea temperature, and salinity, covering the entire North Sea, developed by the Danish Hydraulic Institute (DHI) (Danish Hydraulic Institute 2012).

For hindcast generation, the MIKE 3 Flow Model Flexible Mesh (MIKE3 FM) (Danish Hydraulic Institute 2014) has been set up. The model domain is shown in Fig. 1 taken from

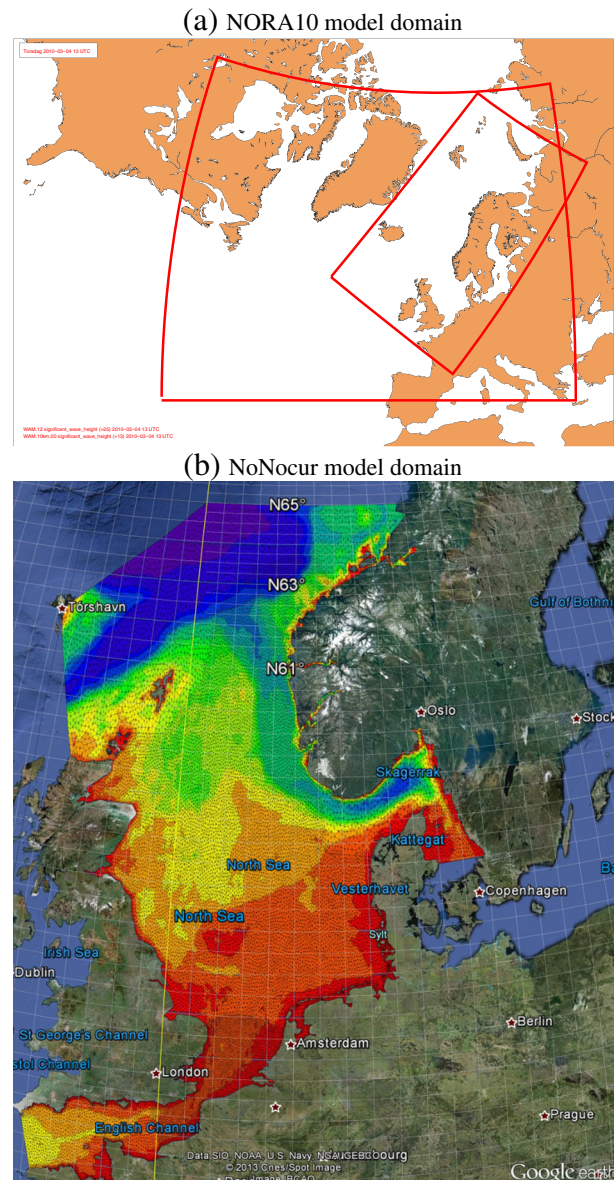


**Fig. 1** **a** Model domains for the NORA10 hindcast. The *outer box* indicates the WAM50 model domain and the *inner box* the HIRLAM10 and WAM10 model domains (which are identical). The *inner box* is also the NORA10 hindcast domain. **b** Model domain for the NoNoCur hindcast. The colored are shows the bathymetry and grid. The figure is taken from the NoNoCur report provided by Statoil from DHI in 2012

the NoNoCur report provided to Statoil (Danish Hydraulic Institute 2012). The atmospheric forcings of the current model are wind speed and direction, air temperature, and pressure from NORA10 and cloud cover, humidity, and precipitation from Climate Forecast System Reanalysis (CFSR) (Chawla et al. 2013; Saha et al. 2010). The ocean forcings are current speed and direction, sea surface height, sea temperature, and salinity from the Mercator ocean circulation model with data assimilation version GLORYS2V1 (Ferry et al. 2012). No additional large-scale currents are applied as boundary



conditions. The model output of the hindcast data is 1 h. The model has an internal time step of 6.8 s. As for NORA10, the time step gives an instant value for this exact point of time and not a mean value during a longer time interval. Yet, the data output from the model every hour is regarded as 10-min mean values (personal communication Morten Rugbjerg at DHI).

NoNoCur covers the period from January 2008 to December 2012 and also 13 storm periods during January 1993 to December 2007. No sophisticated methods were used to define the storm periods; periods with high wind speeds for more than 1 day and known severe strong storms have been selected.

The model has been calibrated against current measurements at five locations in the northern North Sea during May through July 2011. The current measurements cover the entire water column and are sampled every 10 min.

### 2.3 Wave measurements

Wave measurements overlapping with parts of the NORA10 hindcast period are available at several locations in the North Sea. Recently, metocean measurements of wave and current during May 2011 to October 2015, i.e., 4.5 years, at four locations in the central northern North Sea, within the area  $59^{\circ}$  N– $61.5^{\circ}$  N and  $2^{\circ}$  E– $3.5^{\circ}$  E, have been completed. Originally, the measurement program consisted of wave and current measurements at five locations. As the measurements at location number 3 were terminated early, the measurements from this location are not included in this paper, i.e., only measurements at location 1, 2, 4, and 5 are considered. A detailed description of these measurements can be found in Bruserud and Haver (2016, unpublished). Waves have been measured by an Oceanor Wavescan Buoy, which among others measures  $H_s$ ,  $T_p$ , and mean direction. The sample interval is 30 min, with 1024 samples per burst of 17 min, i.e., approximately one sample per

**Fig. 2** Scatter and qq-plots of measured and NORA10 wave data. **a–b** Location 1, **c–d** Location 2, **e–f** Location 4 and **g–h** Location 5

second. This sampling frequency is sufficient when statistical wave parameters such as  $H_s$  and  $T_p$  are the main focus and also to measure individual waves with periods of about 5 s and above, but may not be frequent enough if the details of steep crests are to be investigated. In Table 1, a detailed overview of the wave measurements and the corresponding hindcast information is given. The hindcast data have been selected from the grid point closest to where measurements have been done. The overlapping period of measured and hindcast wave data range from May 2011 to June 2015, i.e., approximately 49 months.

In order to make comparisons between wave measurements and hindcast data as consistent as possible, one wave measurement every 3 h is selected from buoy measurements. In addition, hindcast data is selected only from the time steps when measured data are available, ensuring identical sample sizes of data for comparison.

### 2.4 Current measurements

Current measurements overlapping with parts of the NoNoCur hindcast period are only available at the four locations in the northern North Sea mentioned previously. Comparisons are done at all these locations. The current measurements used for comparison with hindcast are performed with an upward looking RDI 150 kHz Quartermaster ADCP (QM ADCP) placed in a seabed mooring 12 m above the seabed. The sample interval is 10 min, with time per acoustic ping set to 10 s. The data is seen to contain a lot of “noise” resulting in spikes in the data. Due to this, the data have been filtered by a running mean in order to obtain 1-h mean values.

**Table 1** Overview of wave and current measurements and corresponding hindcast information

Parameter	Type	Location	$\Delta$ longitude [ $^{\circ}$ E]	$\Delta$ latitude [ $^{\circ}$ N]	Depth [m]	Period	Time step [h]	Measurement depths [m]	
Waves	Measurements	1	0	0	190	04 May 2011–04 October 2015	0.5 (30 min)	Sea surface	
		2			100				
		4			118				
		5			125				
		NORA10			1				0.018
	2	–0.002	0.060						
	4	0.132	–0.002						
	5	0.315	–0.370						
	Current	Measurements	1	0	0	190	04 May 2011–04 October 2015	0.167 (10 min)	Every 2 m from 3 to 43 m
			2			100			Every 10 m from 26 to 106 m
4			118			Every 1 m from 1 m above seabed to 9 m above seabed			
5			125						
NoNoCur			1			–0.002			–0.023
2		–0.032	0.018	90					
4		–0.018	0.018	100			Every 10 m from surface to 90 m		
5		0.105	–0.010	100			Every 10 m from surface to 100 m		

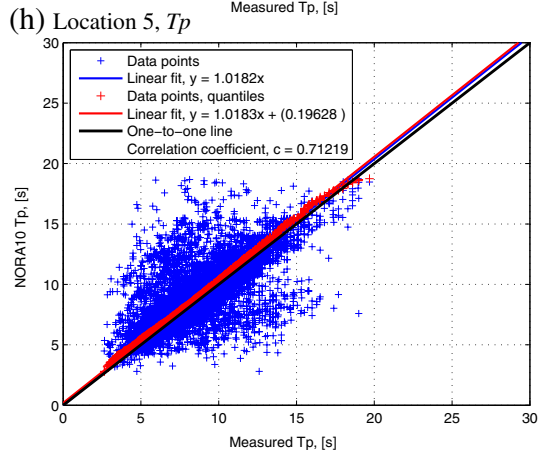
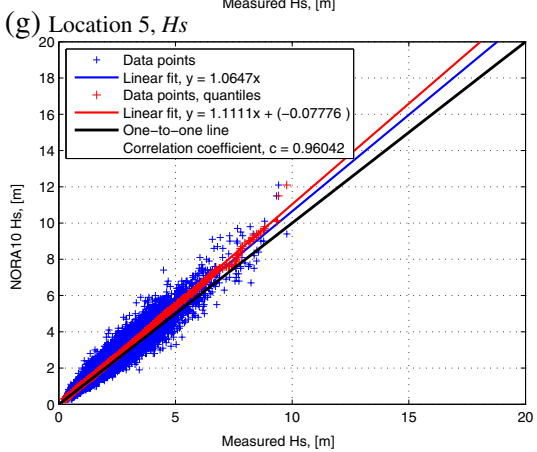
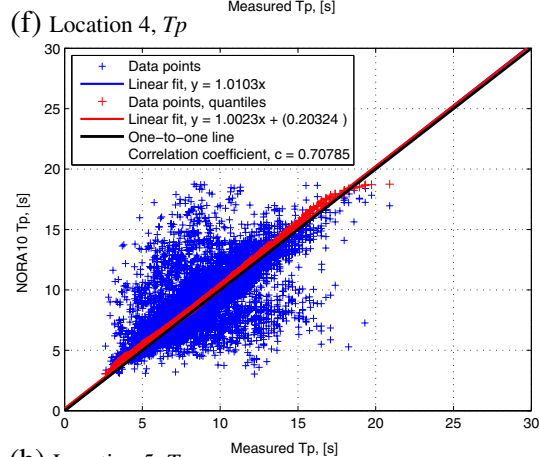
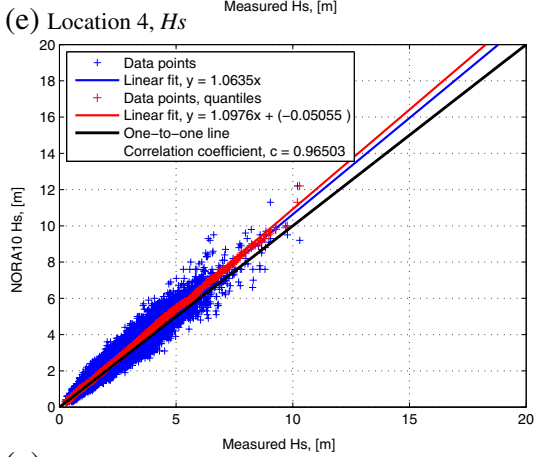
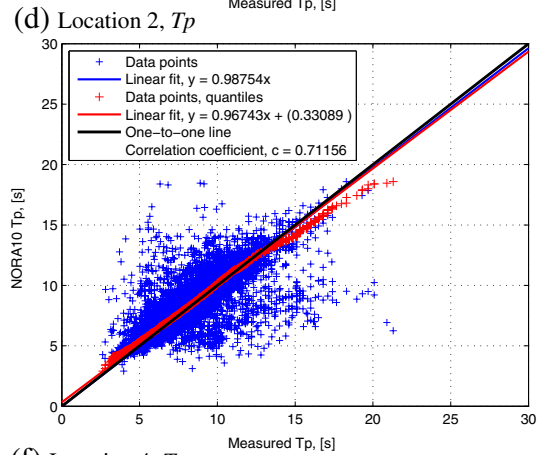
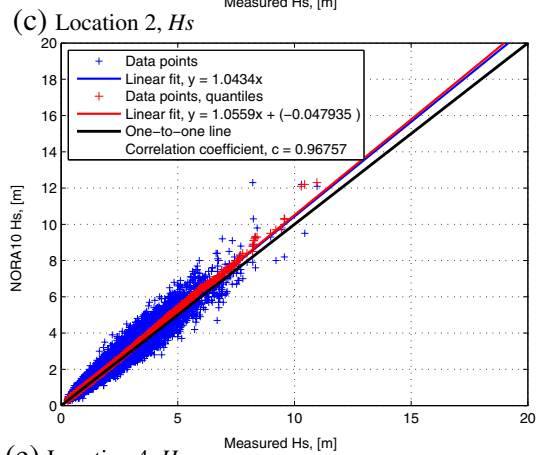
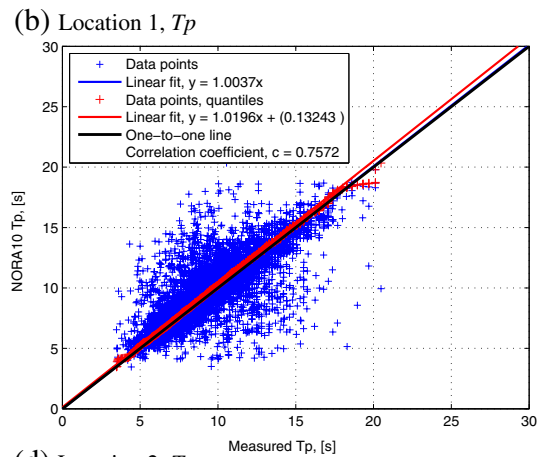
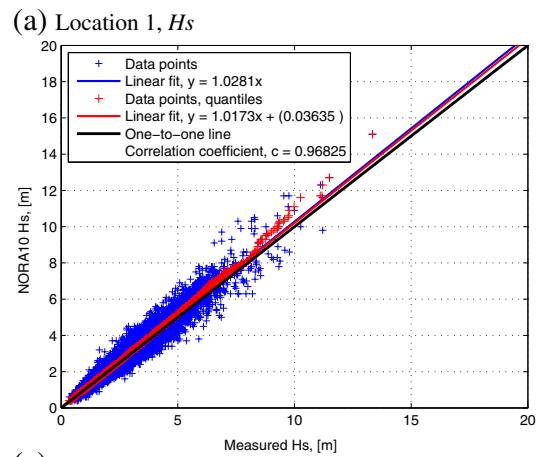


**Fig. 3** The wave rose based on measured wave data and NORA10 at **a–b** Location 1, **c–d** Location 2, **e–f** Location 4 and **g–h** Location 5. The wave direction, measured in degrees clockwise from north, is the direction from which the waves are coming

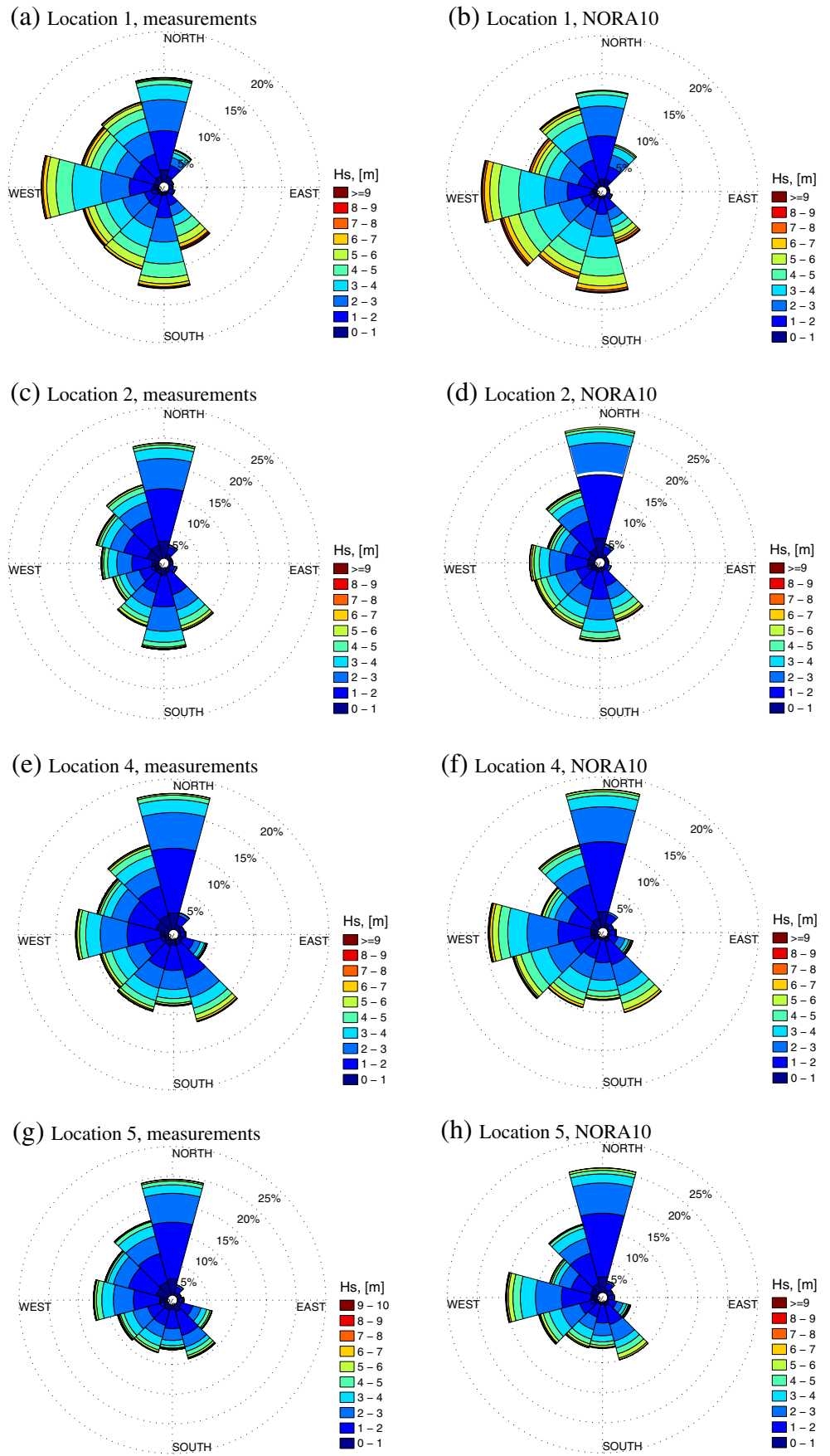


**Table 2** Summary wave statistics

$H_s$	Location	Data	0°	30°	60°	90°	120°	150°	180°	210°	240°	270°	300°	330°	Omni	
Sample distribution [%]	1	Measurements	14.2	4.8	0.6	0.6	0.8	7.7	12.7	10.8	10.4	15.5	10.8	11.0	100.0	
		NORA10	13.1	6.2	0.4	0.4	0.7	5.9	13.1	11.3	13.2	15.4	9.6	10.6	100.0	
	2	Measurements	19.6	2.6	0.6	0.7	1.4	10.2	13.9	10.1	8.1	9.6	10.7	12.5	100.0	
		NORA10	22.1	2.6	0.6	0.6	1.1	8.9	12.4	10.5	10.5	10.9	8.2	11.5	100.0	
	4	Measurements	18.4	2.7	0.8	1.0	3.7	11.4	8.9	10.0	9.5	12.5	9.8	11.5	100.0	
		NORA10	18.6	2.3	0.9	1.1	3.2	10.5	8.3	9.7	11.6	14.8	8.0	11.2	100.0	
	5	Measurements	19.8	2.0	0.8	1.1	5.8	9.5	7.5	8.4	8.6	12.6	11.1	12.8	100.0	
		NORA10	21.1	2.3	1.1	1.1	3.7	10.0	7.7	7.9	10.1	15.3	8.4	11.5	100.0	
	Mean [m]	1	Measurements	2.2	2.1	1.4	1.9	1.7	3.7	3.1	3.3	3.4	3.2	3.0	2.8	2.6
			NORA10	2.1	2.1	1.5	1.6	1.8	3.4	3.5	3.4	3.6	3.3	3.1	2.9	2.7
2		Measurements	1.9	1.4	1.3	1.5	1.6	2.6	2.3	2.6	2.5	2.4	2.2	2.2	2.0	
		NORA10	1.9	1.4	1.5	1.7	1.8	2.9	2.5	2.7	2.8	2.5	2.4	2.2	2.2	
4		Measurements	2.0	1.4	1.3	1.4	2.2	2.6	2.4	2.6	2.7	2.4	2.1	2.3	2.1	
		NORA10	1.9	1.3	1.4	1.5	2.6	2.8	2.6	2.9	2.9	2.7	2.3	2.3	2.3	
5		Measurements	1.9	1.4	1.5	1.7	2.5	2.3	2.2	2.5	2.5	2.4	1.9	2.1	2.1	
		NORA10	1.9	1.3	1.5	1.6	2.6	2.7	2.5	2.8	2.8	2.6	2.1	2.0	2.2	
Maximum [m]		1	Measurements	10.0	6.2	4.8	4.8	4.2	9.6	10.3	8.3	13.4	9.8	11.2	11.1	13.4
			NORA10	5.6	5.8	2.4	3.3	3.3	9.3	10.2	8.1	11.7	15.1	10.3	12.3	15.1
	2	Measurements	6.9	5.1	3.5	4.6	5.3	8.3	9.6	8.2	8.3	11.0	10.4	7.5	11.0	
		NORA10	6.1	5.2	5.1	5.5	3.6	8.0	8.2	7.8	10.3	12.3	10.3	8.2	12.3	
	4	Measurements	6.7	4.3	4.2	4.9	8.5	9.1	8.8	8.8	9.7	10.2	10.3	9.8	10.3	
		NORA10	6.6	3.0	2.5	3.3	9.3	8.2	7.6	9.3	10.0	12.2	9.9	7.6	12.2	
	5	Measurements	6.8	4.0	4.6	4.2	9.8	8.8	8.4	7.9	9.4	9.4	8.8	7.6	9.8	
		NORA10	6.5	4.1	3.7	4.4	9.4	8.2	7.7	9.3	10.1	12.1	10.1	7.6	12.1	

A detailed overview of the current measurements and corresponding hindcast information is given in Table 1. The overlapping period of measured and hindcast current data is from 04 May 2011 to 31 December 2012, i.e., 20 months. Note that

the measured current data used to calibrate the NoNoCur model (May to July 2011) is included in the measured current data.

As for wave data, only simultaneous current measurements and hindcast data are selected for comparison, i.e., one current

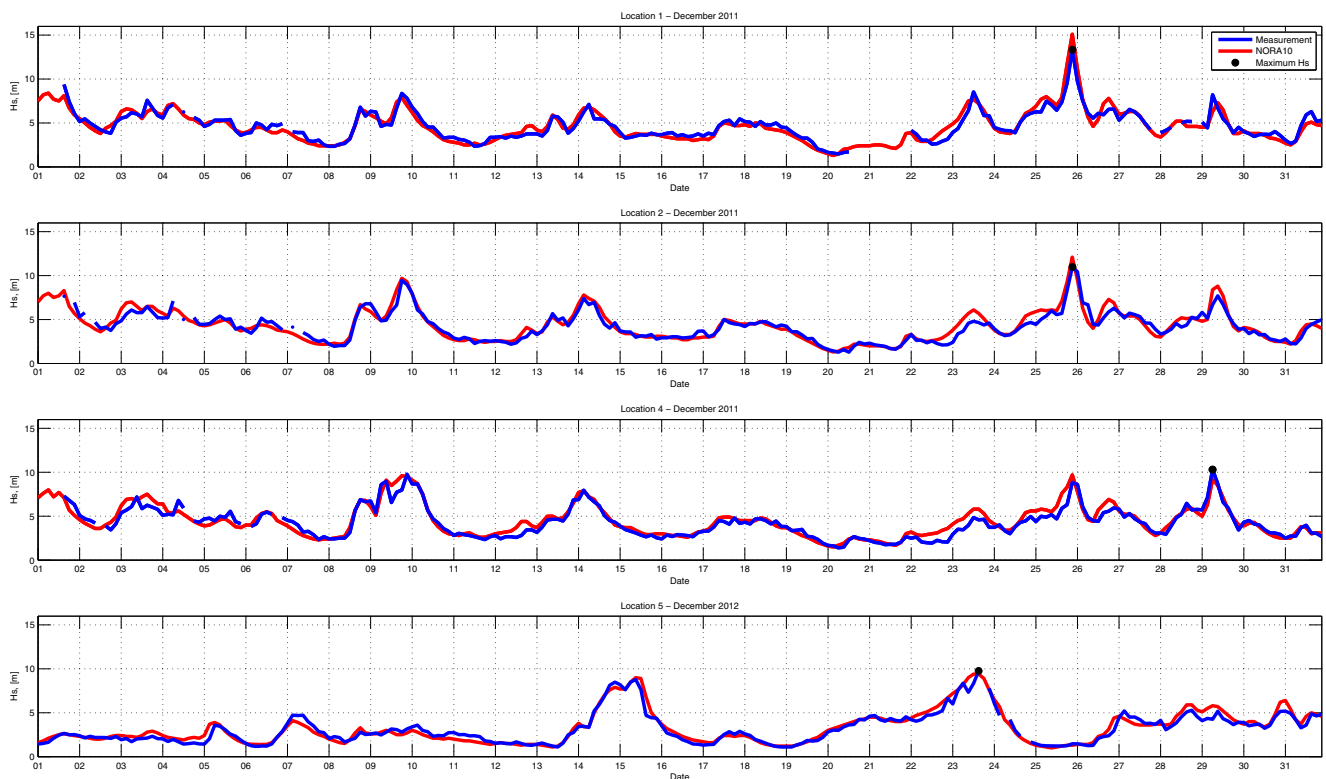


**Fig. 4** Time series of measured and NORA10  $H_s$  for selected months

measurement every hour and hindcast data only at time steps where measured data is available.

Over the last decade, acoustic current meters, such as the QM ADCP, have to a large extent taken over for mechanical instruments for current velocity measurements. Confidence in current measurements performed with different instruments and technologies depends on consistency between these. Recently, current measurements performed with different acoustic and mechanical current meters at the same water depths have become available. Discrepancies are observed, and following this, the quality of current measurements is questioned (Bruserud and Haver, 2016, unpublished). Further investigations are ongoing and will be presented in a separate, future paper.

### 3 Results

#### 3.1 Wave measurements and NORA10 hindcast

Scatter and qq-plots of  $H_s$  and  $T_p$  for measured and NORA10 hindcast wave data at the four locations in the northern North

Sea are shown in Fig. 2. The scatter and qq-plots of  $H_s$  at all the four locations show good agreements. The estimated correlation coefficient at all locations, ranging between 0.96 and 0.97, also supports this. However, the NORA10 data seems to be somewhat more conservative than the measured data. There is an indication of a north-south difference in this conservatism. The linear fit to the data is considered to be very good and indicates the conservatism in the NORA10 data to be around 3 to 6 %, assuming the measurements to be the ground truth. But uncertainties are present also in the measurements, so there is no robust reason for correcting hindcast  $H_s$ .

The scatter plots of  $T_p$  show a much larger spread in the data than for  $H_s$ , which is also reflected in the correlation coefficient ranging between 0.70 and 0.75. This is probably explained by the difficulties in deciding the peak of the wave spectrum when there is more than one wave system in the wave hindcast model, e.g., one wind sea system and one or two swell systems. The qq-plots of  $T_p$  agree quite well. The linear fits to both  $T_p$  data and quantiles are very close to the one-to-one line.

The roses for measured and NORA10  $H_s$  are given in Fig. 3 and the corresponding summary wave statistics in Table 2. The

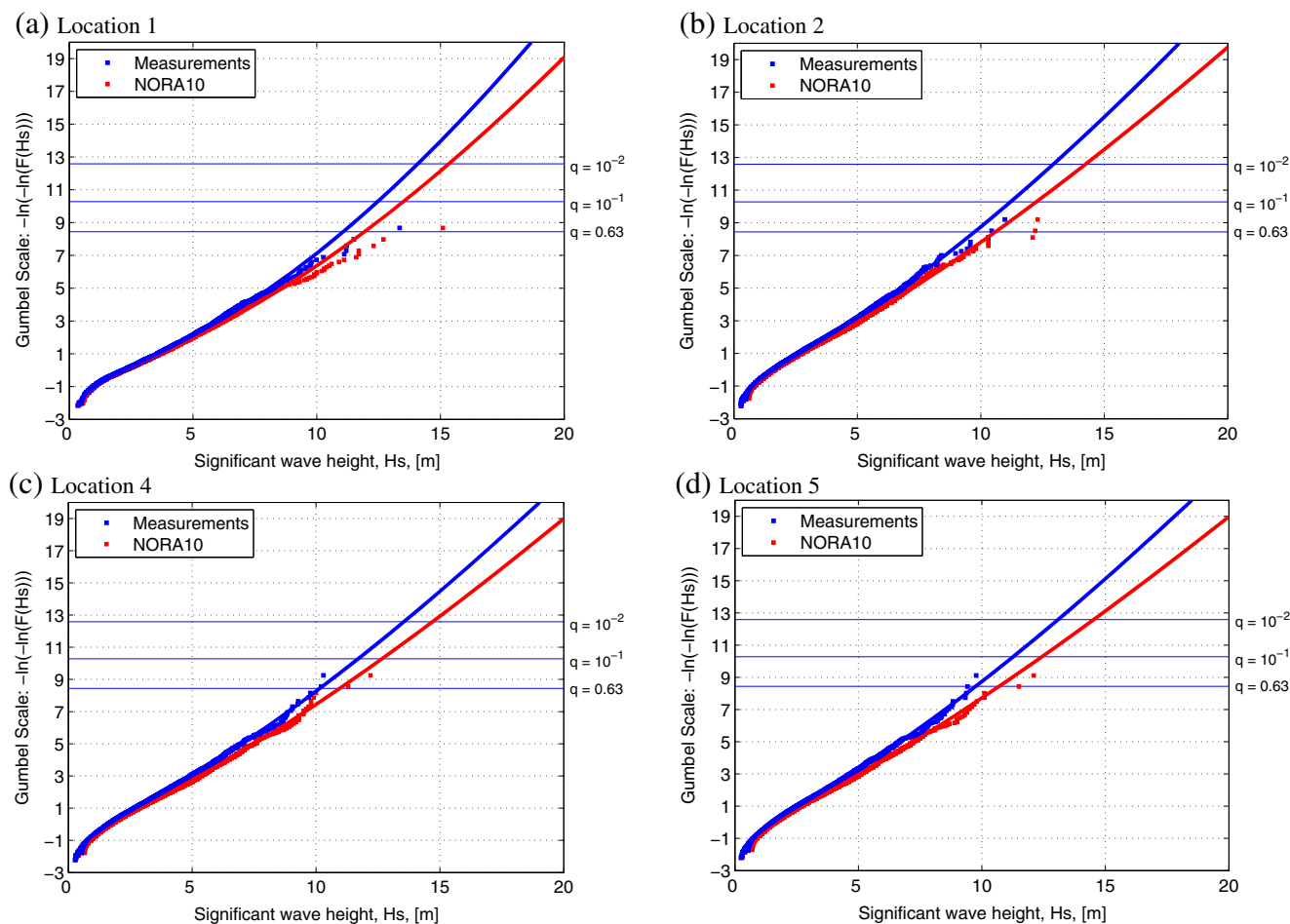


**Fig. 5** Empirical (squares) and fitted (lines) distributions of  $H_s$  for wave measurements (blue) and corresponding NORA10 hindcast (red) at **a** Location 1, **b** Location 2, **c** Location 4 and **d** Location 5



**Table 3** Weibull parameters and corresponding extreme values for  $H_s$  [m]

Location	Data	Weibull parameters			Annual probability of exceedance		
		$\gamma$	$\beta$	$\alpha$	0.63	$10^{-1}$	$10^{-2}$
1	Measurements	1.592	2.77	0.49	11.1	12.5	14.1
	NORA10	1.519	2.79	0.56	11.9	13.5	15.3
2	Measurements	1.348	1.90	0.50	9.7	11.2	12.9
	NORA10	1.279	1.88	0.62	10.6	12.2	14.2
4	Measurements	1.317	1.90	0.55	10.1	11.7	13.5
	NORA10	1.286	1.96	0.66	11.0	12.7	14.7
5	Measurements	1.290	1.76	0.55	9.7	11.3	13.1
	NORA10	1.232	1.77	0.70	10.7	12.4	14.5

mean wave direction, measured in degrees clockwise from the north, is the direction from which the waves are coming. In general, the  $H_s$  roses and sample distributions correspond very well at all locations for most directions. Slight differences between measurements and NORA10 are seen at all locations for the sector from the southwest, i.e.,  $225^\circ$  to  $255^\circ$ , and from the northwest, i.e.,  $285^\circ$  to  $315^\circ$ . The discrepancy seen for the southwestern sector seems to correspond to where the Shetland Islands are placed relative to these locations, and a too large sheltering effect of the Shetland Islands could explain the difference. For locations 4 and 5, this effect can explain the difference for the northwestern sector as well, but no similar obvious explanation can be offered for locations 1 and 2. The directional and omnidirectional mean  $H_s$  values are very close and in most cases either identical or deviating with only 0.1 m with NORA10 mean  $H_s$  slightly larger than the measured mean  $H_s$ . Larger deviations in directional maximum  $H_s$  values are seen. The difference in omnidirectional maximum  $H_s$  is between 1.3 and 2.3 m. In general, there are very little data for the eastern and southeastern directions, and quite large differences are seen. This is also evident for previously mentioned western sectors where differences in the directional distributions of measured and NORA10  $H_s$  are observed.

Time histories of  $H_s$  for the month with the maximum measured  $H_s$  at each location, respectively, are shown in Fig. 4. At locations 1, 2, and 4, maximum  $H_s$  was measured in December 2014, while it was measured in December 2012 at location 5. As seen in Fig. 4, some measurements of  $H_s$  during these months are missing and these are just left blank and not interpolated. The correspondence between both wave data sets is good at all four locations, especially when the sea states are low. During the storm periods when measurements of the maximum  $H_s$  are available and when  $H_s$  peak values are exceeding 8 m, NORA10  $H_s$  can be between 1 to 2 m larger than the measured  $H_s$ . This is in accordance with the deviation in omnidirectional maximum  $H_s$  seen in Table 2. No obvious explanation can be offered and further investigation is required.

The long-term distribution of  $H_s$  has been modeled in terms of a three-parameter Weibull distribution, and the

parameters were estimated by the method of moments (Bruserud and Haver 2015). Figure 5 shows the empirical and fitted Weibull distributions of  $H_s$ . Deviations are seen in the upper part of the empirical distributions where  $H_s$  is larger than 8 m, with the NORA10 data more conservative than the measured wave data. This is in accordance with the scatter, qq-plots, and also time histories in Figs. 2 and 4. Table 3 shows the Weibull parameters and the corresponding extreme values of  $H_s$  for measured and hindcast data. The duration of the sea states is set to 3 h. The difference in the estimated extreme values follows from the differences in the empirical distributions. Such a deviation in estimated extreme values based on measured and hindcast data, respectively, is quite concerning as this can introduce unnecessary conservative  $H_s$  values for design. However, when bootstrapping of 100 data samples from the fitted Weibull distribution to measured data at location 4 is performed, it is seen that the fitted Weibull distribution to NORA10 data falls within the natural range

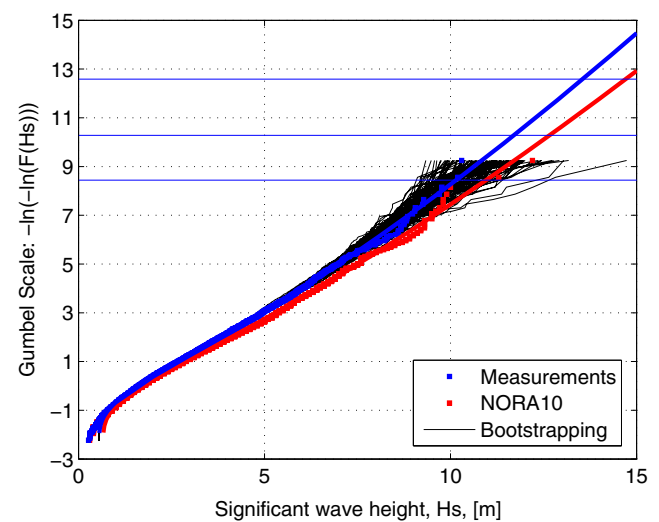


**Fig. 6** Empirical (squares) and fitted (lines) distributions of  $H_s$  for wave measurements (blue) and corresponding NORA10 hindcast (red). The black lines are 100 bootstrapped samples from the fitted distribution of  $H_s$  to wave measurements

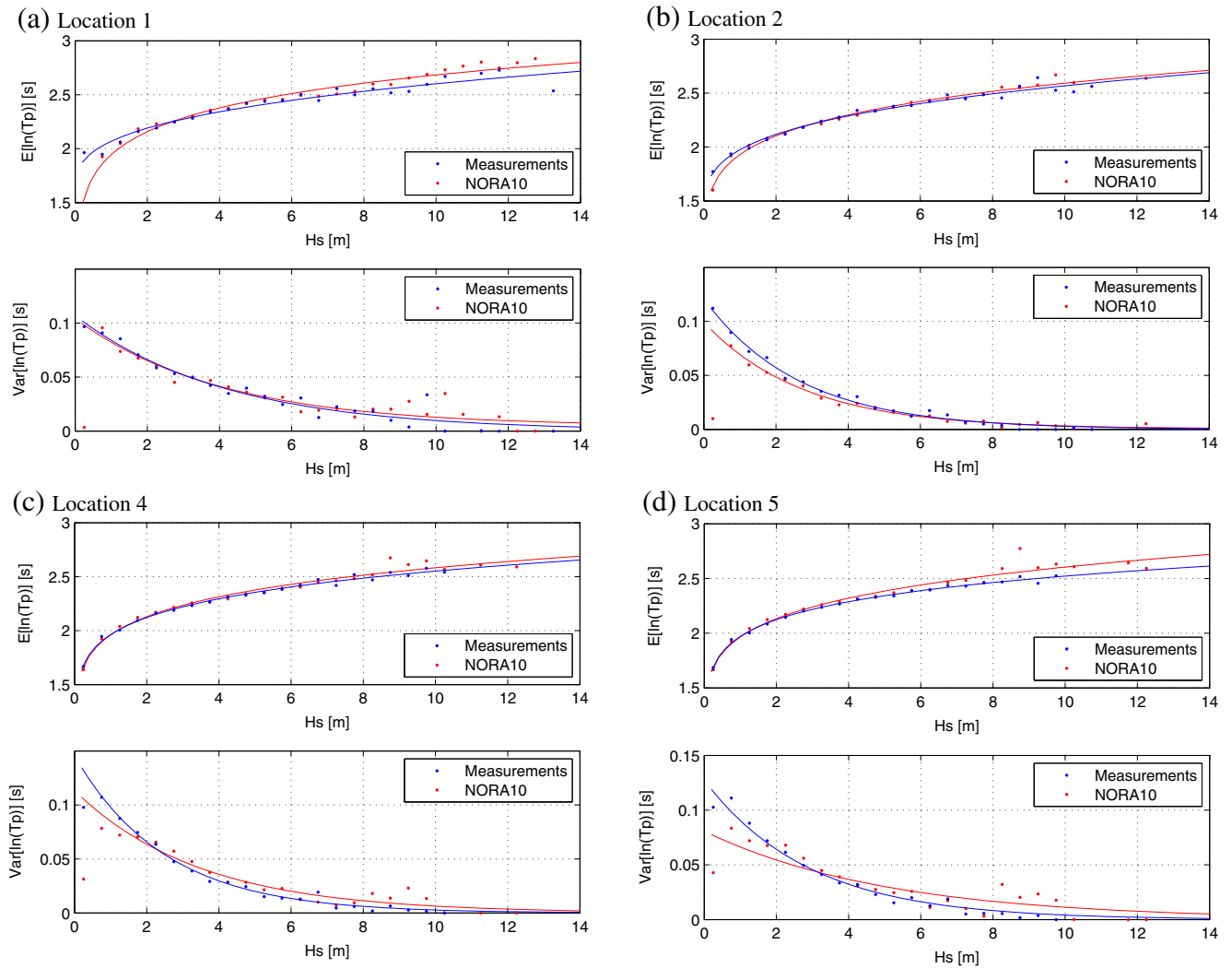


**Fig. 7** Estimated  $E[\ln(T_p)]$  and  $\text{Var}[\ln(T_p)]$  given  $H_s$  and fitted distributions of wave measurements compared to NORA10 at **a** Location 1, **b** Location 2, **c** Location 4 and **d** Location 5

of variability for the measured data (see Fig. 6). Until more measured data become available, no correction of hindcast  $H_s$  is recommended.

**Table 4** Parameters for the fitted conditional log-normal distribution of  $T_p$  given  $H_s$

Location	Data	Parameters					
		$a_1$	$a_2$	$a_3$	$b_1$	$b_2$	$b_3$
1	Measurements	1.58	0.489	0.058	0	0.100	0.240
	NORA10	-3.25	5.200	0.320	0.0043	0.107	0.248
2	Measurements	1.27	0.703	0.265	0	0.121	0.374
	NORA10	0.49	1.440	0.164	0.00055	0.099	0.362
4	Measurements	0.36	1.830	0.127	0	0.105	0.346
	NORA10	0.13	1.610	0.136	0	0.125	0.249
5	Measurements	-0.20	2.170	0.098	0	0.103	0.343
	NORA10	0.63	1.330	0.170	0.0011	0.127	0.261

### 3.2 Conditional distribution of $T_p|H_s$

The joint probability density distribution of  $H_s$  and  $T_p$  is given by

$$f_{H_s, T_p}(h_s, t_p) = f_{H_s}(h_s) f_{T_p|H_s}(t_p|h_s) \tag{1}$$

where  $f_{H_s}(h_s)$  is a log-normal Weibull distribution and  $f_{T_p|H_s}(t_p|h_s)$  a log-normal distribution as described by Haver (1985):

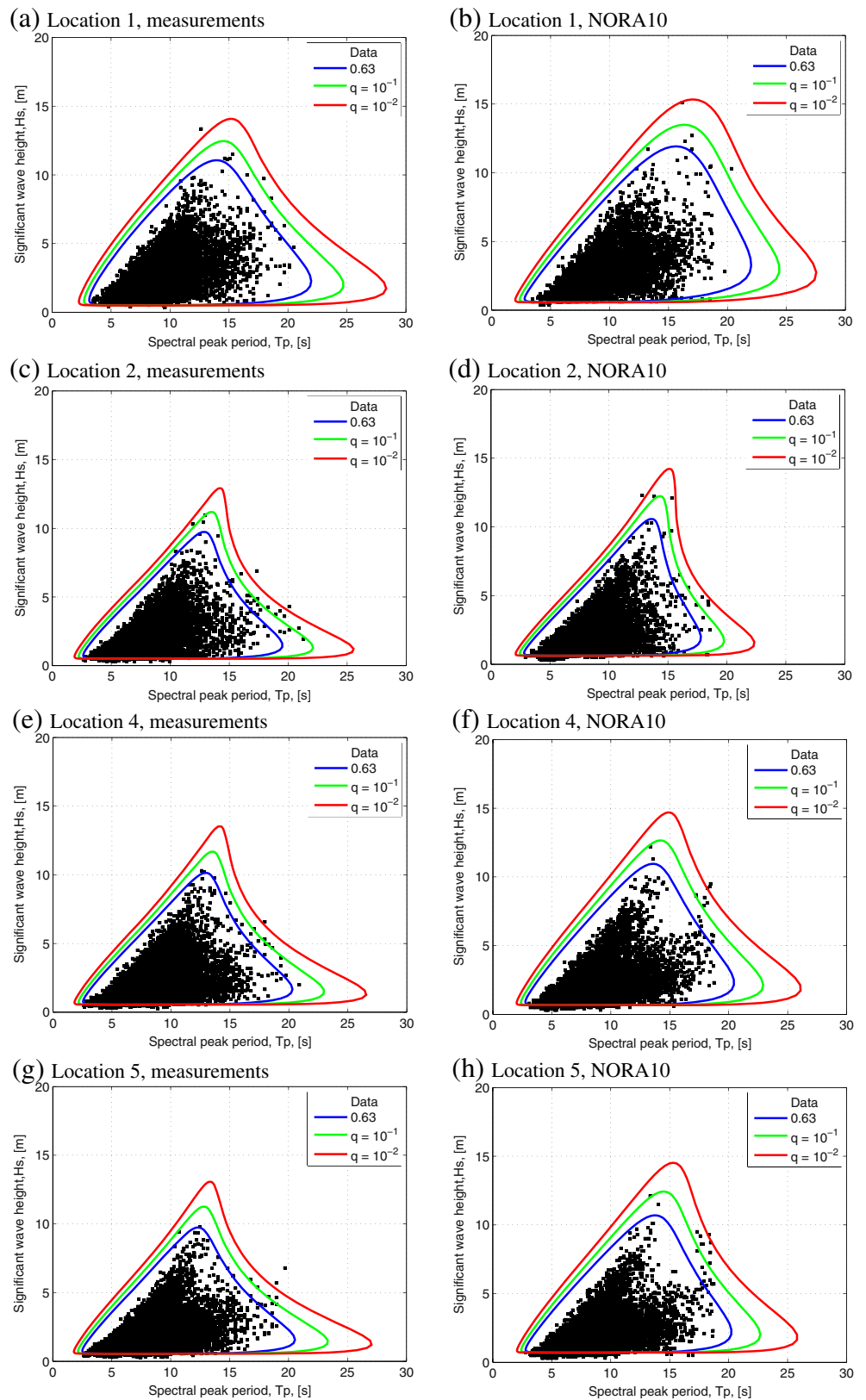
$$f_{H_s}(h_s) = \frac{1}{\sqrt{2\pi}\vartheta h_s} \cdot \exp\left[-\frac{1}{2}\left(\frac{\ln(h_s)-\theta}{\vartheta}\right)^2\right] \text{ for } h_s \leq \alpha \tag{2}$$

$$f_{H_s}(h_s) = \frac{\gamma}{\beta} \left(\frac{h_s}{\beta}\right)^{\gamma-1} \exp\left[-\left(\frac{h_s}{\beta}\right)^\gamma\right] \text{ for } h_s > \alpha \tag{3}$$

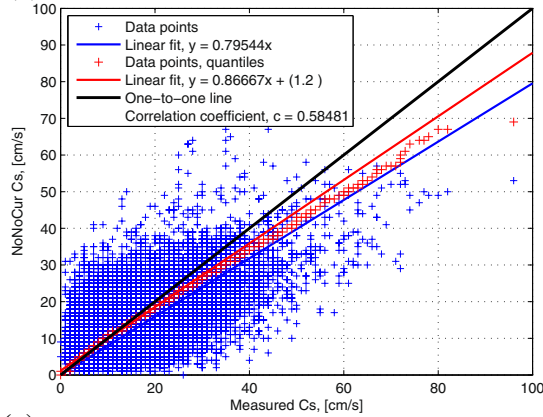
and

$$f_{T_p|H_s}(t_p|h_s) = \frac{1}{\sqrt{2\pi}\sigma t_p} \cdot \exp\left[-\frac{1}{2}\left(\frac{\ln(t_p)-\mu}{\sigma}\right)^2\right] \tag{4}$$

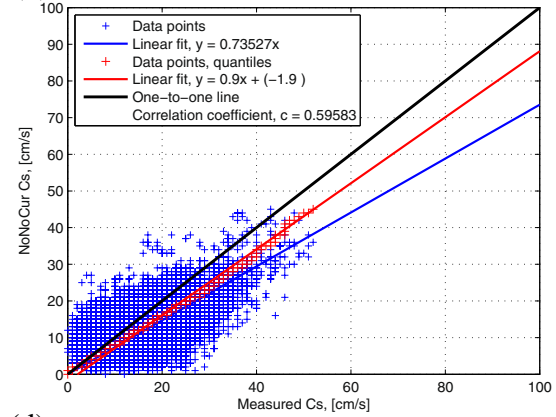
**Fig. 8** Contour lines of  $H_s$ - $T_p$  with annual probability of exceedance 0.63,  $10^{-1}$ , and  $10^{-2}$  for wave measurements and NORA10 data at **a–b** Location 1, **c–d** Location 2, **e–f** Location 4 and **g–h** Location 5. Duration of sea state is set to 3 h



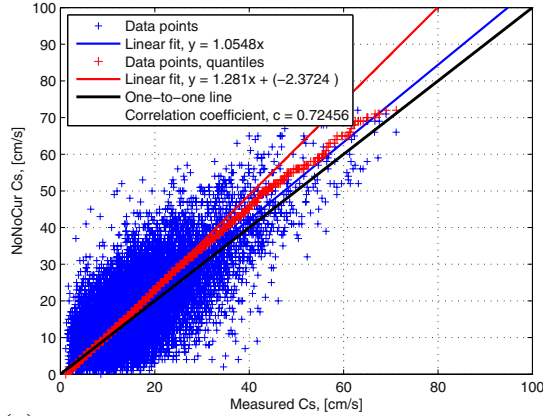
(a) Location 1, 40 m



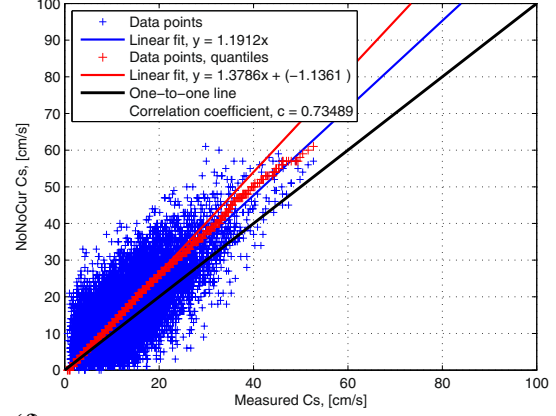
(b) Location 1, 3 m above seabed



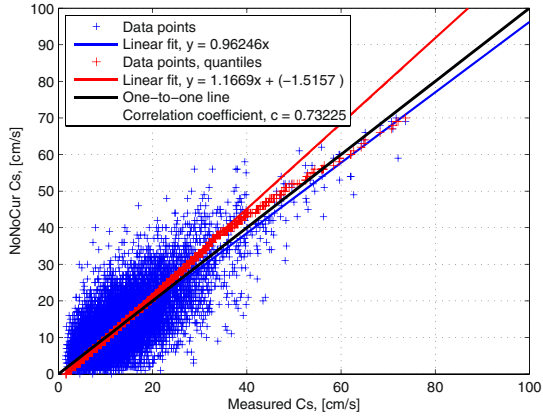
(c) Location 2, 40 m



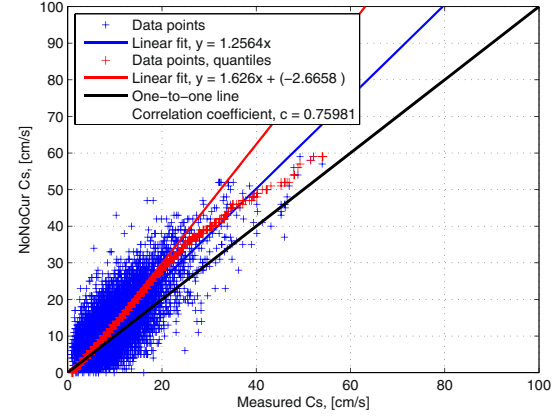
(d) Location 2, 3 m above seabed



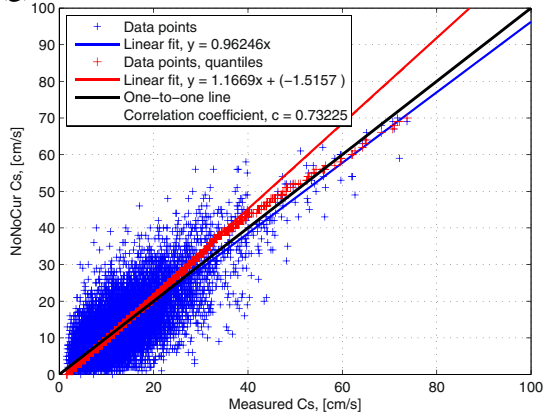
(e) Location 4, 40 m



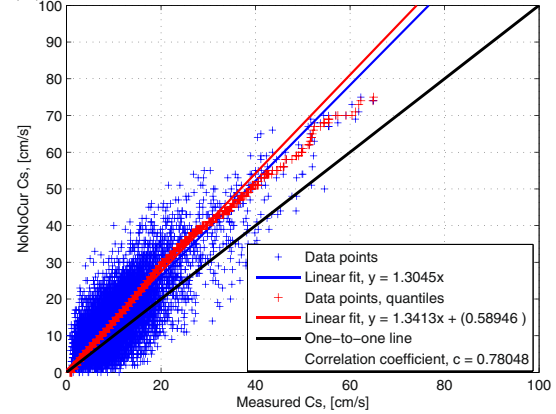
(f) Location 4, 3 m above seabed



(g) Location 5, 40 m



(h) Location 5, 3 m above seabed



◀ **Fig. 9** Scatter qq-plots of measured and NoNoCur  $C_s$  for two selected water depths at **a–b** Location 1, **c–d** Location 2, **e–f** Location 4 and **g–h** Location 5

where

$$\mu = a_1 + a_2 h_s^{a_3} \tag{5}$$

$$\sigma^2 = b_1 + b_2 \exp(-b_3 h_s) \tag{6}$$

In order to ensure a positive variance,  $\sigma^2$ , the best practice for the NCS is to set the parameter  $b_1$  to 0.005. This was originally based on a relatively short time period (late 1970s to early 1980s) of wave observations in northern North Sea, consisting of 20-min measurements recorded every 3 h. Since first proposed and recommended, the conditional distribution of  $T_p$  given  $H_s$  has not been revisited and is still in use. However, it is often argued that the  $b_1$  value of 0.005 is too large. When more wave data, both measurements and hindcast, for a much longer

**Fig. 10** Current roses at 40-m water depth at **a–b** Location 1, **c–d** Location 2, **e–f** Location 4 and **g–h** Location 5. The current direction, measured in degrees clockwise from the north, is the direction toward which the current is flowing

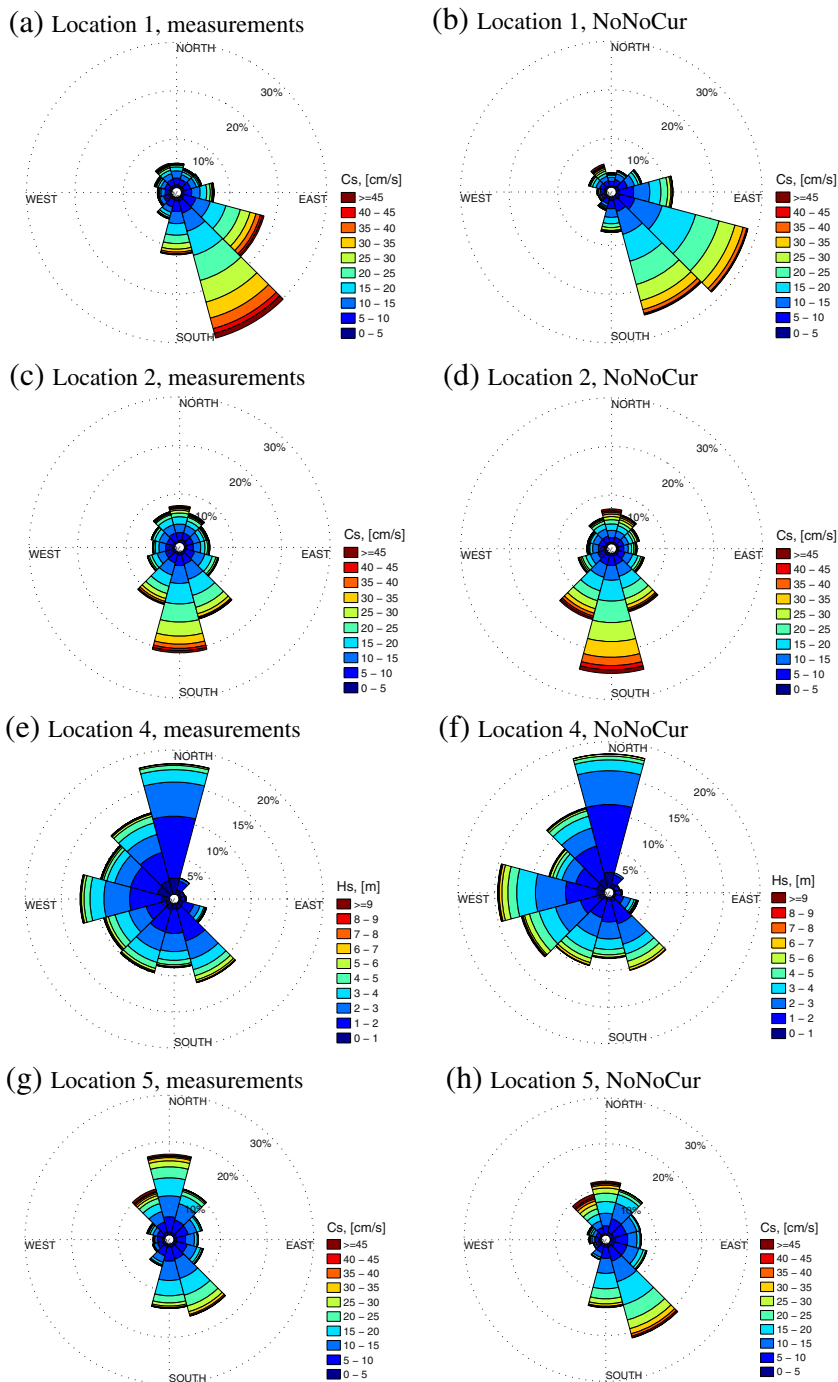




**Table 5** Summary current speed statistics at 40-m water depth

$C_s$ [cm/s]	Location	Measurement	Hindcast
Mean	1	17.8	16.3
	2	16.6	18.8
	4	13.5	13.5
	5	14.4	14.8
Maximum	1	96.0	69.0
	2	71.1	72.0
	4	73.7	70.0
	5	92.9	77.0
Standard deviation	1	11.2	9.2
	2	9.4	11.1
	4	7.2	8.1
	5	8.6	9.1

period and at more locations have become available, it is possible to investigate the  $b_1$  value further.

Figure 7 shows the estimated  $E[\ln(T_p)]$  and  $\text{Var}[\ln(T_p)]$  given  $H_s$  and the fitted distributions for wave measurements compared to NORA10 at all four locations. The corresponding parameters for the fitted conditional log-normal distribution of  $T_p$  given  $H_s$  is given in Table 4. The only restriction on  $b_1$  is that this cannot be negative, and if so,  $b_1$  is set to 0 and the parameters  $b_2$  and  $b_3$  are estimated again. In general, the fitted distributions are good and measured data compares quite well to NORA10. At locations 1 and 5, the NORA10 data are seen to give larger expected conditional  $T_p$  than the measurements, while the expected conditional  $T_p$  is considered identical at locations 2 and 4. The variance conditional  $T_p$  compares well, but some deviations between measurements and NORA10 are evident at locations 4 and 5. For wave measurements,  $b_1$  is 0 at all locations and the NORA10  $b_1$  0.0043 at location 1, 0.00055 at location 2, 0 at location 4, and 0.0011 at location 5, i.e., larger than the corresponding wave measurement  $b_1$  value though close to 0. The length of the wave measurement and thus the corresponding NORA10 data are probably too short to capture the real variation in  $T_p$ . Based on these results, it is likely that  $b_1$  can be somewhat reduced from 0.005 for the North Sea. Further investigations regarding the effects of this change should be investigated for long-term response analysis and the metocean contour method approach for estimating extremes.

Contour lines of  $H_s-T_p$  are given in Fig. 8. Compared to wave measurements, the contour lines based on NORA10 hindcast data are slightly less sharp-pointed. When the contour method is used to select appropriate sea states for model tests, this difference in contour lines might affect the selection of percentile level. At the NCS, the percentile level is normally set to 90 % when  $b_1$  equal to 0.005 is used.

### 3.3 Measurements of currents and NoNoCur hindcast

The scatter and qq-plots for measured and hindcast  $C_s$  at two selected depths, one near the surface at 40 m and one near the seabed at 3 m above the seabed, are shown in Fig. 9.

The scatters at 40-m water depths at locations 2, 4, and 5 are quite good and the correlation coefficient is ranging from 0.72 to 0.75. The linear fits follow the one-to-one line closely and deviate up to 5 % only, which is considered to be very good for current measurements and hindcast comparisons. However, the comparison between NoNoCur hindcast data and current measurement is far from as good as for NORA10 hindcast data and wave measurements. One plausible explanation for this may be that modeling of waves in these areas has been focused on and worked with over a longer period and thus both knowledge and skills with wave modeling are more advanced than for current modeling. At location 1, there are more spread in the data and the correlation coefficient and linear fit are only 0.58 and 0.795, respectively. For the qq-plots at 40 m, the NoNoCur hindcast  $C_s$  is seen to be more conservative than the measured  $C_s$  at locations 2, 4, and 5 but nonconservative at location 1. The deviation in quantile linear fit from the one-to-one line is ranging from -14 to 28 %.

Near the seabed, both scatter and qq-plots show that the NoNoCur data are more conservative than the measured current data at locations 2, 4, and 5 and less conservative at location 1. However, the correlation coefficients at all locations have approximately the same values as at 40 m. The linear fit to data is deviating between 20 and 30 % from the one-to-one line at locations 2, 4, and 5 and at location 1 around -24 %. A larger deviation in the linear fit to quantiles from the one-to-one line near the seabed than at 40 m is also seen. If the measured current data (May through July 2011) used to calibrate the NoNoCur hindcast data are removed, the scatter and qq-plots at the selected water depths are unchanged, i.e., this has no effect on the scatter and qq-plots. The poorer agreement between measured and NoNoCur data 3 m above the seabed compared to the other water depth is probably due to a difference in total water depth; NoNoCur data at location 1 is from 200 m, location 2 from 90 m, and locations 4 and 5 from 100-m water depth and not exactly 3 m above the seabed, i.e., 190, 100, 118, and 125 m for the different locations, respectively. Based on this, further analysis and comparison of current data 3 m above the seabed is not done.

The measured and NoNoCur  $C_s$  roses at 40-m water depth are given in Fig. 10. The current direction, measured in degrees clockwise from the north, is the direction toward which the current is flowing. The directional current distributions are comparable for both data sets at all locations and have the same shape/main features. A general observation is that NoNoCur have more  $C_s$  exceeding 30 cm/s than the measurements, which also supports the observation of the NoNoCur data being more conservative than the measurements.

Summary current statistics are given in Table 5. There are no evident trends in either the mean or maximum  $C_s$  values at 40-m water depth. At location 1, the measured mean and maximum values are larger than the NoNoCur values. At location 2, the mean NoNoCur value is larger than the measured, while the maximum values are comparable. At location 4, both mean and maximum values are comparable. At location 5, the mean values are similar, but the measured maximum value is larger than the NoNoCur value. The standard deviation of NoNoCur  $C_s$  is generally larger than for measured  $C_s$  at locations 2, 4, and 5, but at location 1, this is reversed.

Time histories of  $C_s$  at 40-m water depth for the month with the maximum observed  $C_s$  at each location are shown in Fig. 11. At locations 1, 2, and 4, the maximum observed  $C_s$  was in January 2012, and at location 5, this was in December 2012. In general, at locations 2, 4, and 5, the correspondence between measured and NoNoCur  $C_s$  is very good during the entire period. The timing of  $C_s$  variations in NoNoCur data compared to measurements is excellent. Some differences are seen in the  $C_s$  values, but despite this, the  $C_s$  values are considered to be quite comparable. Very surprisingly, the measured and NoNoCur  $C_s$  values agree excellently at and around the maximum measured  $C_s$  values at locations 2 and 4. At location 1, the NoNoCur and measured  $C_s$  values do not compare very well.

In all the different types of comparisons of NoNoCur to measured  $C_s$ , the comparisons at location 1 deviate from the

comparisons at the three other locations. Location 1 is located in the Norwegian Trench further north in the North Sea than the other locations, at a significantly larger water depth. In the central North Sea, the current conditions are mainly wind-driven currents. At location 1, Atlantic inflow might influence the current conditions. Thus, the poorer agreement between NoNoCur and measured  $C_s$  at location 1 can be an indication of different governing current conditions at this location than at the three other locations further south.

Based on the previously mentioned observed discrepancies between current measurements performed with different acoustic and mechanical current meters at the same water depths, it is difficult to decide whether the current measurements or NoNoCur hindcast gives the most correct description of the current conditions. However, in order to establish good current hindcasts such as NoNoCur, current measurements will always be needed for validation and tuning of the hindcast model. It might not be unreasonable to assume that the “true” current conditions are somewhere in between the current measurements and NoNoCur hindcast.

### 4 Conclusions

Wave measurements at four locations in the northern North Sea during May 2011 to October 2015 have been compared to simultaneous NORA10 wave hindcast data. In general, good

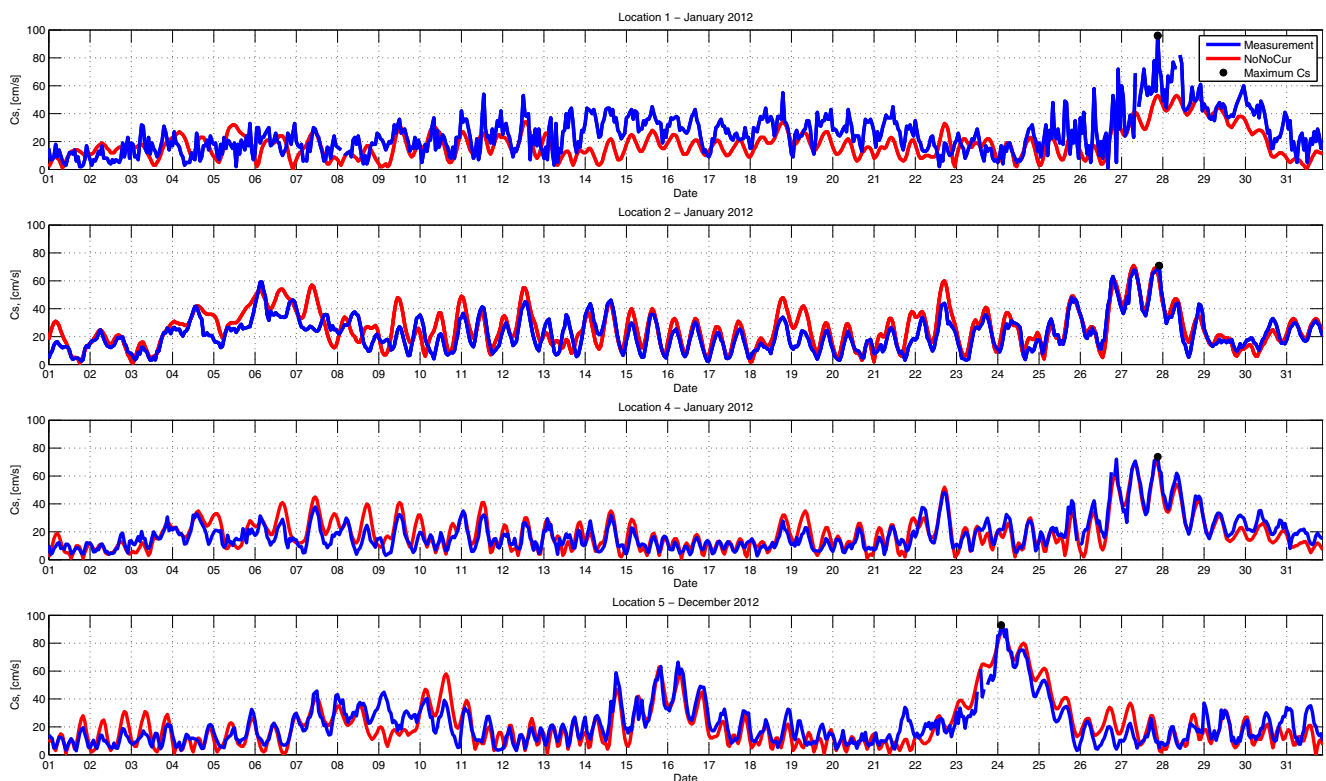


Fig. 11 Time series of  $C_s$  at 40-m water depth

agreements are found between measured and hindcast data at all four locations.

Current measurements at the same locations in the northern North Sea have been compared to NoNoCur hindcast data at two selected water depths. The correspondence between measured and hindcast  $C_s$  is considered to be very good for a current hindcast, especially at locations 2, 4, and 5 in the central northern North Sea. At location 1, located at a larger water depth in the Norwegian Trench further north compared to the other three locations, the current hindcast and measurements do not compare as well. This is probably explained by the general current conditions being somewhat influenced by the Atlantic inflow.

However, this current hindcast is not as good as the wind and wave hindcast for the northern North Sea and must be used with caution. Further work and improvements are required and a good starting point would be to extend the hindcast for a longer continuous period and also to test how the current hindcast performs under extreme wind conditions.

**Acknowledgments** This work was made possible by funding from the Norwegian Research Council's Industrial PhD-program (231832) and from Statoil. Sincere gratitude is expressed to chief engineer Simen Moxnes who secured Statoil's funding. Statoil and Norwegian Deepwater Program (NDP) are acknowledged for the permission to use the data and publish these results. Thanks to Magnar Reistad (Norwegian Meteorological Institute) for patient answers to NORA10 questions and to Ole Johan Aarnes (Norwegian Meteorological Institute) for providing Fig. 1a. Morten Rugbjerg (Danish Hydraulic Institute) is thanked for good answers to questions related to NoNoCur hindcast data and permission to publish Fig. 1b. The authors are thankful to two anonymous reviewers for their helpful comments on an earlier version of the manuscript.

## References

Aarnes OJ, Breivik Ø, Reistad M (2012) Wave extremes in the northeast Atlantic. *J Clim* 25:1529–1543. doi:10.1175/JCLI-D-11-00132.1

- Bruserud K, Haver S (2015) Effects of waves and currents on extreme loads on a jacket. *J Offshore Mech Arctic Eng*. doi:10.1115/1.4031099
- Chawla A, Spindler DM, Tolman HL (2013) Validation of a thirty year wave hindcast using the Climate Forecast System Reanalysis winds. *Ocean Model* 70:189–206. doi:10.1016/j.ocemod.2012.07.005
- Danish Hydraulic Institute (2012) Northern North Sea current hindcast (NoNoCur). Danish Hydraulic Institute, Hørsholm
- Danish Hydraulic Institute (2014) Mike 21 & Mike 3 flow model FM, hydrodynamic and transport module, scientific documentation. Danish Hydraulic Institute, Hørsholm
- Dee DP et al (2011) The ERA-Interim reanalysis: configuration and performance of the data assimilation system. *Q J R Meteorol Soc* 137: 553–597. doi:10.1002/qj.828
- Ferry N et al. (2012) GLORYS2V1 global ocean reanalysis of the altimetric ERA (1993–2009) at Meso scale. *Mercator Ocean Q Newsletter*:28–39
- Francis PE (1987) The North European Storm Study (NESS). 1987/1/1/
- Furevik BR, Haakenstad H (2012) Near-surface marine wind profiles from rawinsonde and NORA10 hindcast. *J Geophys Res Atmos* 117 doi:10.1029/2012JD018523
- Günther H, Hasselmann S, Janssen PAEM (1992) The WAM model cycle 4. Deutsche KlimaRechnenZentrum, Hamburg
- Haver S (1985) Wave climate off northern Norway. *Appl Ocean Res* 7: 85–92
- Komen GJ, Cavaleri L, Donelan M, Hasselmann K, Hasselmann S, Janssen PAEM (1996) Dynamics and modelling of ocean waves. Cambridge University Press, Cambridge
- Oceanweather Inc (2014) Nextra\_A5 summary report., Next JIP
- Oceanweather Inc. (2016) Global reanalysis of ocean waves 2012 (GROW2012) project description
- Peters DJ, Shaw CJ, Grant CK, Heideman JC, Szabo D (1993) Modelling the North Sea through the North European Storm Study. 1993/1/1/
- Reistad M, Breivik Ø, Haakenstad H, Aarnes OJ, Furevik BR, Bidlot JR (2011) A high-resolution hindcast of wind and waves for the North Sea, the Norwegian Sea, and the Barents Sea. *J Geophys Res Oceans* 116
- Saha S et al (2010) The NCEP climate forecast system reanalysis. *Bull Am Meteorol Soc* 91:1015–1057. doi:10.1175/2010BAMS3001.1
- The Wamdi Group (1988) The WAM model—a third generation ocean wave prediction model. *J Phys Oceanogr* 18:1775–1810. doi:10.1175/1520-0485(1988)018<1775:TWMTO>2.0.CO;2
- Undén P et al (2002) HIRLAM-5 scientific documentation. Swedish Meteorological and Hydrological Institute, Norrköping
- Uppala SM et al (2005) The ERA-40 re-analysis. *Q J R Meteorol Soc* 131:2961–3012. doi:10.1256/qj.04.176